J. Fluid Mech. (1989), *vol.* 207, *pp.* 323–352
Printed in Great Britain

Heating a salinity gradient from a vertical sidewall: linear theory

By OLIVER S. KERR
School of Mathematics, University of Bristol, Bristol, BS8 1TW, UK

(Received 12 May 1988 and in revised form 30 November 1988)

When a body of fluid with a vertical salinity gradient is heated from a single vertical wall, instabilities have sometimes been observed experimentally (Thorpe, Hutt & Soulsby 1969; Chen, Briggs & Wirtz 1971; Tsinober & Tanny 1986). We present a linear stability analysis for this configuration and show that for strong salinity gradients the stability of the fluid to infinitesimal disturbances is governed by a single non-dimensional parameter,

$$Q = \frac{(1-\tau)^6 g(\alpha \Delta T)^6}{\nu \kappa_S l^2 (-\beta \bar{S}_z)^5}$$

where g is the acceleration due to gravity, α the coefficient of thermal expansion, β the density change due to a unit change in the salinity, ΔT the change of temperature at the wall, $\bar{S}_z$ the vertical salinity gradient, l the horizontal lengthscale $(\kappa_T t)^{\frac{1}{2}}$, ν the kinematic viscosity, κ_T the diffusivity of heat, κ_S the diffusivity of salt and τ the salt/heat diffusivity ratio. This non-dimensional parameter is related to the Rayleigh number, however, it involves two different lengthscales; the penetration depth of the thermal front, l, and the height by which a heated element of fluid would rise in the salinity gradient, $g\alpha\Delta T/(-\beta\bar{S}_z)$. This analysis is valid when the ratio of the vertical lengthscale to the horizontal lengthscale is small. This analysis gives good agreement with the published experimental results.

1. Introduction

In this paper we investigate the stability of a semi-infinite body of fluid with a vertical salinity gradient that has been heated or cooled from a sidewall. In this situation the heat will only penetrate a finite distance into the fluid, and there will be a non-uniform lateral temperature gradient. This contrasts with the previous theoretical work on the effect of horizontal compositional gradients in double-diffusive systems which have assumed linear gradients in the background state, with the possible exception of thin boundary layers at the wall which do not play a significant role in the dynamics. The previous work can be subdivided into two main categories. The first of these is concerned with infinite bodies of fluid with linear gradients. This work is usually motivated by oceanic applications and often includes the effect of vertical rotation. In this category there have been used a variety of different models for the diffusion of heat and salt, for example eddy diffusivities (Stern 1967; Toole & Georgi 1981), eddy-flux coefficients (McDougall 1985) or molecular diffusivities (Kerr & Holyer 1986). The second main category that has been studied is concerned with the instabilities observed between two parallel walls. These walls may be vertical or inclined. The first theoretical study of the instabilities found when a vertical salinity gradient in a vertical slot is subjected to a temperature difference between the walls is due to Thorpe, Hutt & Soulsby (1969) under the

approximation that, in some sense, the salinity gradient is strong. This linear analysis of a vertical slot has been extended by Hart (1971) and Thangam, Zebib & Chen (1981). The case of instabilities in an inclined slot has been looked at by Chen (1975), Chen & Sandford (1977) and Paliwal & Chen (1980*a*, *b*). Chen looked at the evolution of the background flow of an inclined slot with a vertical salinity and temperature gradient and no flux conditions at the walls. The stability of this time dependent background flow was then investigated, both numerically and experimentally by Chen & Sandford. The case of an inclined slot containing a fluid with a vertical salinity gradient and an imposed temperature difference between the two walls was examined experimentally and theoretically in Paliwal & Chen (1980 *a*, *b*).

Thorpe, Hutt & Soulsby also conducted a series of experiments for a narrow vertical slot. In addition they also presented the results of an experiment with a wide slot. When one of the walls was heated, instabilities were observed before the heat had penetrated to the far wall of the slot. This configuration, effectively heating a semi-infinite fluid from a single sidewall, was studied by Chen, Briggs & Wirtz (1971) in experiments that examined the marginal stability of the fluid. More recently Tsinober & Tanny (1986) (see also Tanny & Tsinober 1988) conducted a more detailed experimental investigation of the marginal stability of a similar experimental configuration. In Tsinober & Tanny's analysis of their experimental results they used a comparison with the theoretical results of Thangam *et al.* for a finite slot of width $(\kappa_T t)^{\frac{1}{2}}$, the distance that the heat had penetrated due to diffusion since the onset of the experiment. Using theoretical results for a finite slot for comparison with experiments on effectively semi-infinite fluids had previously been done by Linden & Weber (1977) in their study of the instabilities induced by a sloping boundary inserted into a fluid with vertical temperature and salinity gradients. The linear theory presented here agrees well with the experimental results of Chen *et al.* (1971) and of Tsinober & Tanny (1986).

Also of some relevance to the problem under consideration in this paper are the experiments of Huppert & Turner (1980) and Huppert & Josberger (1980) in their investigations into the fluid motions caused by blocks of ice melting into salinity gradients, and the experiments of Huppert, Kerr & Hallworth (1984) in their investigations into convection-layer thickness due to sidewall heating for different values of the Prandtl number and the salt/heat diffusivity ratio. Unlike the experiments of Chen *et al.* (1971) and Tsinober & Tanny (1986) the observed instabilities were far from marginal stability, however they still found that the instabilities observed took the form of thin almost horizontal convection cells with the same basic vertical scaling as that proposed by Chen *et al.* (1971).

The only stability analysis for instabilities due to localized horizontal gradients in a double-diffusive problem is for the piecewise linear temperature and salinity gradients of Niino (1986). This model assumed a steady background state and that the vertical salt and heat fluxes were dominated by the presence of salt fingers. This approach would not be applicable to the case under consideration here since the background salinity gradient is stabilizing, and hence would inhibit the formation of salt fingers.

All the theory that has previously been mentioned, whether for a vertical or inclined slot or for piecewise linear gradients, benefits from the existence of a background state that is uniform in some direction and is independent of time. These background states also have a degree of symmetry about the middle of the slot or, in the case of the Niino model, about the centre of the localized horizontal gradients. This symmetry is also reflected in the perturbations found in the analysis. However,

in the case where a salinity gradient is heated from a single sidewall the symmetry no longer exists and the background flows are, in general, time dependent. In this paper we investigate the linear stability of this time-dependent background flow and compare the results with the published experimental results. In §2 we look at the large-time asymptotic background state for a fluid with a vertical salinity gradient that is heated from a single sidewall. The stability of the background state is investigated in §3, where we show that for a strongly stratified fluid there is only one important non-dimensional number that governs the stability of the fluid. In §4 we compare the results of this linear theory with the available experimental results in the literature. Finally in §5 we look at the effect of the boundary layer near the wall and how the quasi-static assumption made in §3 breaks down.

This paper is only concerned with the linear analysis of the instabilities. The analysis of some of the nonlinear effects are dealt with in Kerr (1989).

2. Background state

In this section we find how a semi-infinite stratified fluid, with a vertical wall, adjusts to a change in the temperature of the wall. Linden & Weber (1977), in their investigations of the effect of a sloping wall in a stratified fluid, found that a steady flow, that was uniform along the boundary, did not exist when the stratification of the fluid was caused by both temperature and salinity gradients unless the diffusivities of heat and salt are the same. In a similar fashion we can look for a steady solution for the background flow that is uniform along the wall for the case of heating a semi-infinite body of fluid with a vertical salinity gradient from a vertical sidewall. The time-dependent governing equations for the vertical velocity, w, of a Boussinesq fluid whose motion is uniform along the wall and for the perturbations to the background temperature and salinity, T and S, for such a flow in a fluid with uniform vertical temperature and salinity gradients $\bar{T}_z$ and $\bar{S}_z$ are

$$\frac{\partial w}{\partial t} = g(\alpha T - \beta S) + \nu \frac{\partial^2 w}{\partial x^2}, \tag{2.1a}$$

$$\frac{\partial T}{\partial t} + w\bar{T}_z = \kappa_T \frac{\partial^2 T}{\partial x^2}, \tag{2.1b}$$

$$\frac{\partial S}{\partial t} + w\bar{S}_z = \kappa_S \frac{\partial^2 S}{\partial x^2}, \tag{2.1c}$$

with the density of the fluid, ρ, given by

$$\rho = \rho_0(1 - \alpha T + \beta S). \tag{2.2}$$

Here ν is the kinematic viscosity, g the acceleration due to gravity, κ_T the diffusivity of heat, κ_S the diffusivity of salt, α the coefficient of thermal expansion and β is the density change due to a unit change in the salinity.

If the wall temperature is increased by ΔT and the salinity by ΔS, it can be shown that for a steady background flow to exist the following condition must be satisfied:

$$\frac{\kappa_T \Delta T}{\bar{T}_z} = \frac{\kappa_S \Delta S}{\bar{S}_z}. \tag{2.3}$$

This condition is not in general satisfied and so, in general, there is no steady solution. Instead we must look at the time-dependent problem. We will confine

ourselves to the case where the vertical stratification is due only to a salinity gradient, so $\bar{T}_z = 0$. Initially the fluid is at rest and both the fluid and the wall are at temperature $T = 0$. At time $t = 0$ the wall temperature is increased by the heating of the wall. This situation matches the experiments that have been performed. The salt boundary condition at the wall could be either that the salt takes a prescribed value at each point on the wall or that there is no salt flux at the wall.

By the use of Laplace transforms it is found that, for the case where the wall temperature is instantaneously increased to $T = \Delta T$ and the salinity at the wall remains unchanged, the leading-order large-time asymptotic behaviour is given by

$$T = \Delta T \operatorname{erfc}\left(\frac{x}{2(\kappa_T t)^{\frac{1}{2}}}\right), \tag{2.4a}$$

$$w \approx \frac{g\alpha\,\Delta T(1-\tau)\,x}{2N^2(\kappa_T \pi t^3)^{\frac{1}{2}}}\exp\left(-\frac{x^2}{4\kappa_T t}\right)+\frac{g\alpha\,\Delta T}{N}\left(\frac{\tau}{\sigma}\right)^{\frac{1}{2}}\exp(-Mx)\sin(Mx)$$
$$-\frac{2g\alpha\,\Delta T x\cos(Nt)}{N^2(\sigma+\tau)\,(2\pi(\nu+\kappa_S)\,t^3)^{\frac{1}{2}}}\exp\left(-\frac{x^2}{2(\nu+\kappa_S)\,t}\right), \tag{2.4b}$$

$$S \approx \frac{\alpha\,\Delta T}{\beta}\operatorname{erfc}\left(\frac{x}{2(\kappa_T t)^{\frac{1}{2}}}\right)-\frac{\alpha\,\Delta T}{\beta}\exp(-Mx)\cos(Mx)$$
$$-\frac{2\alpha\,\Delta T x\sin(Nt)}{\beta N(\sigma+\tau)\,(2\pi(\nu+\kappa_S)\,t^3)^{\frac{1}{2}}}\exp\left(-\frac{x^2}{2(\nu+\kappa_S)\,t}\right), \tag{2.4c}$$

where the Prandtl number is $\sigma = \nu/\kappa_T$, the salt/heat diffusivity ratio $\tau = \kappa_S/\kappa_T$, and the buoyancy frequency, N, is defined by

$$N^2 = -g\beta\bar{S}_z, \quad \text{and} \quad M^4 = \frac{N^2}{4\kappa_S \nu}. \tag{2.5a, b}$$

These large-time solutions have three parts. The first parts in the expressions for the velocity and the salinity have the same lengthscale as the thermal diffusion. This represents the upwelling of the water so that the negative buoyancy of the saltier water balances the positive buoyancy of the temperature. The first term in the salt equation has a mismatch in the boundary condition at $x = 0$. The upwelling water tries to impose a salt boundary condition of $S = \alpha\,\Delta T/\beta$ at $x = 0$, as opposed to the actual condition assumed here of $S = 0$. The second term is the salt boundary layer that would be obtained by applying a salt difference $\Delta S = -\alpha\,\Delta T/\beta$ at the wall to the background salinity gradient without any temperature effects (see, for example, Gill 1966). Thus this term represents the matching of the salt boundary condition to the salinity profile on the thermal layer scale. The last terms in the expressions for the velocity and salinity are decaying oscillations at the buoyancy frequency that result from the initial impulsive disturbance.

Different salt boundary conditions at $x = 0$ will change some of these results. If a condition that the salt perturbation S be equal to ΔS at $x = 0$ is imposed, then, since the problem is linear, this would result in a change in the amplitudes of the salt boundary layer and the buoyancy frequency terms. This is equivalent to adding the motions due solely to the imposition of the salt boundary condition whilst leaving the wall temperature at the ambient level. Of more interest for the purposes of comparison with experiments is the case of a no-flux condition on the salt ($\partial S/\partial x = 0$ at $x = 0$). In this situation we would have a decaying salt boundary layer (dying off in amplitude as $t^{-\frac{1}{2}}$) and an altered buoyancy frequency term. Neither of these

alterations to the salt boundary condition has any effect on the parts associated with the thermal term.

There are three lengthscales associated with the large-time asymptotics, the thermal lengthscale $(\kappa_T t)^{\frac{1}{2}}$, the salt boundary-layer thickness M^{-1} and the lengthscale associated with the buoyancy frequency terms. The lengthscale of the salt boundary layer is time independent, while that of the thermal layer is growing with time. These two lengthscales will separate when

$$M^{-1} \ll (\kappa_T t)^{\frac{1}{2}}. \tag{2.6}$$

For typical experiments (cf. Chen, Briggs & Wirtz 1971) this would give the condition

$$t \gg 1 \text{ s}. \tag{2.7}$$

Since the time taken for the instabilities to appear is normally of the order of a few minutes when the system is marginally stable, this condition is normally satisfied.

It is also possible to look at the response to different temperature boundary conditions at the wall. In the experiments of Chen *et al.* (1971) their wall temperatures did not increase instantaneously but increased to a final temperature over a timescale of some minutes. Their measurements of the wall temperatures as a function of time was well fitted by a time-dependent wall temperature of the form

$$T_{\text{wall}}(t) = \begin{cases} \Delta T(1-\mathrm{e}^{-st}) & (t \geqslant 0), \\ 0 & (t < 0). \end{cases} \tag{2.8}$$

The temperature profile associated with this wall temperature can again be calculated by using a Laplace transform of the temperature equation. The resultant temperature profile is

$$T(x,t) = \Delta T\left[\operatorname{erfc}\left(\frac{x}{2(\kappa_T t)^{\frac{1}{2}}}\right) - \mathrm{e}^{-st}\operatorname{Re}\left\{\exp\left(\mathrm{i}\left(\frac{sx^2}{\kappa_T}\right)^{\frac{1}{2}}\right)\operatorname{erfc}\left(\frac{x}{2(\kappa_T t)^{\frac{1}{2}}} + \mathrm{i}(st)^{\frac{1}{2}}\right)\right\}\right]. \tag{2.9}$$

Tsinober & Tanny (1986) also heated the wall to conform to this temperature evolution. In addition they conducted some experiments with the wall temperature increasing linearly with time after the start of the experiment. In this case the temperature profile that results is given by

$$T = ct\left(\left(1+\frac{x^2}{\kappa_T t}\right)\operatorname{erfc}\left(\frac{x}{2(\kappa_T t)^{\frac{1}{2}}}\right) - \frac{x}{2(\kappa_T t\pi)^{\frac{1}{2}}}\exp\left(-\frac{x^2}{4\kappa_T t}\right)\right), \tag{2.10}$$

where c is the rate of change of wall temperature.

As with the error function temperature profile these two profiles have matching horizontal salinity gradients induced to cancel out the horizontal density gradient to leading order.

For all time-dependent wall temperatures that tend to a constant value ΔT for large time, the temperature profile in the fluid will always tend towards the error-function profile generated by the step change in the temperature. For this reason we will use the error function as the representative temperature and salinity profile for most of the following work.

3. Linear stability analysis

Having found how the stratified fluid responds to an increase in the wall temperature we now investigate the stability of this background state. To make any

progress we have to make some assumptions. The higher-order terms in the large-time asymptotic approximation to the background flow found in the previous section are smaller than the leading-order terms by a factor of order $(Nt)^{-2}$ where t is the elapsed time since the onset of the heating, and N, the buoyancy frequency. In the near marginal experiments of Chen *et al.* (1971) the instabilities are first observed several minutes after the heating of the wall started, while the buoyancy frequency of the fluid was around 1–3 s^{-1}, and so at the onset of instability $(Nt)^{-2}$ is very small. The background flow will then be well described by the leading-order large-time asymptotics. These large-time asymptotics are made up of three distinct parts, a thermal layer, a salt boundary layer and a buoyancy frequency term. The instabilities are driven by the region of the fluid with the horizontal temperature and salinity gradients. Since the lengthscale of the salt boundary layer is much less than that of the thermal layer we will assume that the salt boundary layer has negligible effect and can be ignored. We will also neglect the buoyancy frequency terms since they start off small in amplitude and decay away. They also have a frequency much higher than the growth rate of the instabilities and so one can expect that the interactions between them will be negligible.

With these assumptions we have a background state described by

$$\bar{w} = \frac{g\alpha\,\Delta T(1-\tau)\,x}{2(-g\beta\bar{S}_z)\,(\kappa_T\,\pi t^3)^{\frac{1}{2}}}\exp\left[-\frac{x^2}{4\kappa_T t}\right], \tag{3.1a}$$

$$\bar{T} = \Delta T f\left(\frac{x}{(\kappa_T t)^{\frac{1}{2}}}\right), \tag{3.1b}$$

$$\bar{S} = \frac{\alpha\,\Delta T}{\beta} f\left(\frac{x}{(\kappa_T t)^{\frac{1}{2}}}\right) + z\bar{S}_z, \tag{3.1c}$$

where

$$f(x) = \operatorname{erfc}(\tfrac{1}{2}x). \tag{3.2}$$

Hence the linearized equations for small perturbations to this background flow are

$$\frac{\partial}{\partial t}\nabla^2\psi + \bar{w}\frac{\partial}{\partial z}\nabla^2\psi - \frac{\partial^2}{\partial x^2}\bar{w}\frac{\partial\psi}{\partial z} = g\left(\alpha\frac{\partial T}{\partial x} - \beta\frac{\partial S}{\partial x}\right) + \nu\nabla^4\psi, \tag{3.3a}$$

$$\frac{\partial T}{\partial t} - \frac{\partial\psi}{\partial z}\frac{\partial\bar{T}}{\partial x} + \bar{w}\frac{\partial T}{\partial z} = \kappa_T\nabla^2 T, \tag{3.3b}$$

$$\frac{\partial S}{\partial t} - \frac{\partial\psi}{\partial z}\frac{\partial\bar{S}}{\partial x} + \frac{\partial\psi}{\partial x}\bar{S}_z + \bar{w}\frac{\partial S}{\partial z} = \kappa_S\nabla^2 S, \tag{3.3c}$$

where ψ is the stream function for the perturbation velocity with

$$(u, w) = \left(-\frac{\partial\psi}{\partial z}, \frac{\partial\psi}{\partial x}\right). \tag{3.4}$$

We non-dimensionalize these equations with respect to the following quantities

$$T \text{ with respect to } \Delta T, \tag{3.5a}$$

$$S \text{ with respect to } \frac{\alpha\,\Delta T}{\beta}, \tag{3.5b}$$

$$x \text{ with respect to } l = (\kappa_T t)^{\frac{1}{2}}, \tag{3.5c}$$

$$z \text{ with respect to } h = (1-\tau)h' = (1-\tau)\alpha\Delta T(-\beta\bar{S}_z)^{-1}, \tag{3.5d}$$

$$t \text{ with respect to } h^2/\kappa_T, \tag{3.5e}$$

$$\psi \text{ with respect to } \kappa_T l/h. \tag{3.5f}$$

The horizontal and vertical lengthscales are non-dimensionalized with respect to different quantities. The vertical lengthscale is chosen to be $(1-\tau)h'$. This consists of two parts, the $h' = \alpha\Delta t(-\beta\bar{S}_z)^{-1}$ part is the height by which a fluid element would rise in a salinity gradient if its temperature was increased by ΔT, the lengthscale suggested by Chen *et al.* (1971) in their scaling arguments. The $(1-\tau)$ term is introduced for some simplification at a later stage. The horizontal lengthscale is the thickness of the thermal layer of the background state.

The non-dimensional equations that result are

$$\left(\frac{\partial}{\partial t}+\tfrac{1}{2}\delta^2-\tfrac{1}{2}\delta^2 x\frac{\partial}{\partial x}\right)\nabla_m^2\psi+\delta^2\bar{w}(x)\frac{\partial}{\partial z}\nabla_m^2\psi-\delta^4\frac{\partial\psi}{\partial z}\frac{\partial^2}{\partial x^2}\bar{w}(x)=\frac{\tau\sigma Q}{(1-\tau)}\left(\frac{\partial T}{\partial x}-\frac{\partial S}{\partial x}\right)+\sigma\nabla_m^4\psi, \tag{3.6a}$$

$$\left(\frac{\partial}{\partial t}-\tfrac{1}{2}\delta^2 x\frac{\partial}{\partial x}\right)T+\delta^2\bar{w}(x)\frac{\partial T}{\partial z}-\frac{\partial\psi}{\partial z}\frac{\partial f}{\partial x}=\nabla_m^2 T, \tag{3.6b}$$

$$\left(\frac{\partial}{\partial t}-\tfrac{1}{2}\delta^2 x\frac{\partial}{\partial x}\right)S+\delta^2\bar{w}(x)\frac{\partial S}{\partial z}-\frac{\partial\psi}{\partial z}\frac{\partial f}{\partial x}-(1-\tau)\frac{\partial\psi}{\partial x}=\tau\nabla_m^2 S. \tag{3.6c}$$

The following non-dimensional parameters now appear:

$$\left.\begin{aligned} Q &= \frac{(1-\tau)^6 g(\alpha\Delta T)^6}{\nu\kappa_S l^2(-\beta\bar{S}_z)^5}, \quad \delta = h/l, \\ \sigma &= \frac{\nu}{\kappa_T}, \quad \tau = \frac{\kappa_S}{\kappa_T}, \end{aligned}\right\} \tag{3.7}$$

and the operator

$$\nabla_m^2 = \left(\frac{\partial^2}{\partial z^2}+\delta^2\frac{\partial^2}{\partial x^2}\right). \tag{3.8}$$

The non-dimensional background horizontal compositional gradient and vertical velocity terms are

$$\left.\begin{aligned} \frac{\partial\bar{T}}{\partial x} &= \frac{\partial\bar{S}}{\partial x} = f'(x) = \frac{1}{\pi^{\frac{1}{2}}}\exp(-\tfrac{1}{4}x^2), \\ \bar{w}(x) &= \frac{x}{2\pi^{\frac{1}{2}}}\exp(-\tfrac{1}{4}x^2). \end{aligned}\right\} \tag{3.9}$$

The boundary conditions for the stream function imposed at the wall are that the wall is a stream line, and the no-slip condition, hence

$$\psi = \frac{\partial\psi}{\partial x} = 0 \quad \text{when } x = 0. \tag{3.10}$$

As the wall temperature is prescribed there will be no temperature perturbation at the wall. We will also assume that there is no salt flux through the wall. Hence the other two boundary conditions imposed at the wall are

$$T = \frac{\partial S}{\partial x} = 0 \quad \text{when } x = 0. \tag{3.11}$$

Far away from the wall all the disturbances will decay away, so the boundary conditions at infinity are

$$\left.\begin{aligned} &\frac{\partial\psi}{\partial x}\to 0, \quad \frac{\partial\psi}{\partial z}\to 0, \\ &T\to 0, \quad S\to 0 \quad \text{as } x\to\infty. \end{aligned}\right\} \tag{3.12}$$

The $-\frac{1}{2}\delta^2 x(\partial/\partial x)$ terms in the governing equations are caused by the time dependency of the horizontal lengthscale l. The $\frac{1}{2}\delta^2$ term in the stream function equation arises from the time dependent non-dimensionalization of ψ.

Apart from the Prandtl number, σ, and the salt/heat diffusivity ratio, τ, that are non-dimensional measures of the properties of the fluid, there are two other numbers that parameterize the system, δ and Q. The first of these, δ, is the ratio of the vertical and horizontal lengthscales. The other parameter, Q, plays the role of a Rayleigh number. In the normal Rayleigh–Bénard convection between two flat horizontal plates separated by a distance d and with an imposed temperature difference of ΔT the Rayleigh number is defined as

$$Ra = \frac{g\alpha\,\Delta T d^3}{\nu\kappa_T}. \tag{3.13}$$

The meaning of this parameter can be appreciated from, for example, the mechanistic argument from Turner (1973, pp. 208–209). This argument considers a parcel of fluid with dimensions of order d and density perturbation of order $\rho_0\alpha\,\Delta T$ and examines the magnitude of the distance that such a parcel of fluid would travel in the direction of gravity if it is resisted by viscosity and loses its density difference by thermal diffusion. The Rayleigh number is the ratio of this distance to the vertical separation of the plates, and so convection would be expected to occur if this ratio was larger than some order-one number. For the heating of a salinity gradient from a sidewall this argument has to be modified. Firstly, although the appropriate density perturbation will still be $\rho_0\alpha\,\Delta T$ this will be due to anomalies in the temperature and the salinity. The rate at which these anomalies will decrease will be limited by the smaller of the diffusivities of heat and salt. For salt in water κ_S is two orders of magnitude less than κ_T and so will be more important. The other modifications arise from the presence of two lengthscales, the lengthscale, l, of the horizontal temperature and salinity gradients, and the height, h', by which an element of fluid would rise if its temperature was increased by ΔT. Any convection cell that would appear would have height of order h' and length of order l. In the situation we are considering $l \gg h'$ and so h' is the important lengthscale for the diffusive effects. The horizontal lengthscale comes into the problem in two ways. As the height of the convection cells are of order h' and the length of order l the parcels of fluid will not be moving parallel to gravity as in Rayleigh–Bénard convection but along streamlines with slope of order h'/l. This reduces the effective buoyancy force, and hence the distance the parcel of fluid would travel, by a factor of h'/l. Secondly, the distance that the fluid element must travel is of order l and not h'. This introduces another factor of h'/l into the argument. These changes to Turner's argument give a resultant parameter

$$Q' = \frac{g\alpha\,\Delta T h'^5}{\nu\kappa_S l^2} \tag{3.14}$$

which would determine the marginal stability of the flow. This is the same as the parameter that came out of the non-dimensionalization, apart from the extra factor of $(1-\tau)^6$ whose significance will be seen later on in this section.

Although we are using the error-function temperature (and salinity) profile caused

by an instantaneous jump in the wall temperature, in reality the temperature of the wall can take several minutes to heat up and for the fluid to develop instabilities. For a strongly stratified fluid (h is small) this means that δ will be very small when instabilities are first observed. However instabilities will grow exponentially in magnitude with growth rate of order 1 in the non-dimensional units, except for values of Q very close to a critical value. The thermal boundary layer has a growth rate proportional to δ^2 which is equal to $1/t$, the inverse of the non-dimensional time since the start of the wall heating. Hence, for realistic wall heating, δ^2 will be very small and it will change very slowly compared with the growth rate of the instabilities. This leads us to the next assumption that we will make, the quasi-static assumption. We assume that δ^2 can be taken to be a constant, which is equivalent to the statement that

$$\delta^2 \ll 1. \tag{3.15}$$

This quasi-static assumption and its validity will be looked at in more detail in §5.

As we are concerned with the case where δ^2 is very small we could neglect all terms involving it in (3.6). This results in ignoring all the horizontal diffusion terms. Since the flow is driven by the horizontal temperature and salinity gradients in the bulk of the fluid we would expect neglecting these terms to have no effect to leading order. However this model of the flow would cease to be valid in a boundary layer near the wall. We will return to this boundary layer and the effect of a non-zero δ in §5, but suffice it to say that neglecting all the δ^2 terms results in errors of order δ^2. Taking $\delta^2 = 0$, equations (3.6) become

$$\frac{\partial}{\partial t}\frac{\partial^2\psi}{\partial z^2} = \frac{\tau\sigma Q}{(1-\tau)}\left(\frac{\partial T}{\partial x} - \frac{\partial S}{\partial x}\right) + \sigma\frac{\partial^4\psi}{\partial z^4}, \tag{3.16a}$$

$$\frac{\partial T}{\partial t} - \frac{\partial\psi}{\partial z}f'(x) = \frac{\partial^2 T}{\partial z^2}, \tag{3.16b}$$

$$\frac{\partial S}{\partial t} - \frac{\partial\psi}{\partial z}f'(x) - (1-\tau)\frac{\partial\psi}{\partial x} = \tau\frac{\partial^2 S}{\partial z^2}. \tag{3.16c}$$

As horizontal diffusion is not present in these equations we must drop both the boundary conditions that involve this, the no-slip condition for the stream function and the no-flux condition for the salt.

As neither t nor z appear explicitly in these equations we look for solutions that are periodic in the vertical and have an exponential time dependence, i.e. solutions with

$$\psi, T, S \propto \exp(\lambda t + \mathrm{i}mz), \tag{3.17}$$

With this z and t dependence the equations become

$$-\lambda m^2\psi = \frac{\tau\sigma Q}{(1-\tau)}\left(\frac{\partial T}{\partial x} - \frac{\partial S}{\partial x}\right) + \sigma m^4\psi, \tag{3.18a}$$

$$\lambda T - \mathrm{i}m\psi f'(x) = -m^2 T, \tag{3.18b}$$

$$\lambda S - \mathrm{i}m\psi f'(x) - (1-\tau)\frac{\partial\psi}{\partial x} = -\tau m^2 S. \tag{3.18c}$$

We are interested in finding the conditions of marginal stability and so we look for solutions in which the growth rate has no real part, setting

$$\lambda = \mathrm{i}\omega, \tag{3.19}$$

where ω is real. With this z and t dependence we can eliminate both S and T from (3.18) and derive an equation for $\psi(x)$,

$$0 = \psi'' + \frac{\mathrm{i}m^3(\psi f')'}{(\mathrm{i}\omega + m^2)} - \frac{m^2(\mathrm{i}\omega + \tau m^2)(\mathrm{i}\omega + \sigma m^2)}{\tau\sigma Q}\psi, \tag{3.20}$$

with boundary conditions

$$\psi(0) = 0, \quad \psi(x) \to 0 \quad \text{as } x \to \infty. \tag{3.21}$$

From (3.18b) we observe that the statements $\psi = 0$ and $T = 0$ are equivalent, and so the temperature conditions at $x = 0$ and ∞ are both satisfied when ψ satisfies (3.21). Similarly, since $\partial\psi/\partial x \to 0$ as $x \to \infty$, (3.18c) implies that the salinity condition at infinity is also satisfied.

The inclusion of the $(1-\tau)$ factors in the definitions of Q and of the vertical lengthscale, h, means that this factor does not appear in (3.20) and a singularity is removed in the limit $\tau \to 1$. The inclusion of this factor also has the effect that this equation is unchanged if σ and τ are interchanged.

To find non-trivial solutions to (3.20) we have to solve the eigenvalue problem to find values of Q, ω and m for which solutions exist. We first investigate whether or not it is possible to find marginal states with $\omega = 0$. To do this we set $\omega = 0$ in (3.20) and multiply this expression by the complex conjugate of ψ. Then, by integrating from $x = 0$ to ∞ and taking the imaginary part of the resulting expression, we derive the necessary condition for an instability to have $\omega = 0$, that

$$\int_0^\infty |\psi|^2 f'' \,\mathrm{d}x = 0. \tag{3.22}$$

For sidewall heating $f''(x)$ is always positive for any monotonically increasing wall temperature and so this condition can never be satisfied. However an analogous condition will be satisfied for the case of the vertical slot where the temperature profile is linear. In this case the results of Thorpe *et al.* (1969) and Hart (1971) are retrieved in terms of the parameters used here (see Appendix).

For the case that we are interested in, with $f(x) = \mathrm{erfc}\,(\frac{1}{2}x)$, (3.20) cannot be solved directly, instead it was solved numerically using standard techniques over a finite interval with an appropriate radiation condition at the end of the interval away from the wall. The eigenvalues Q and ω corresponding to marginal stability for a range of values of m were found. These values of Q and ω for marginal stability are shown in figure 1 for $\sigma = 7$ and $\tau = \frac{1}{80}$, the approximate values for salt in water. The curve of Q plotted against m has a minimum. This gives the point of marginal stability of the system as a whole. For values of Q less than that of the minimum there are no unstable modes and the fluid is stable to infinitesimal disturbances. For values of Q greater than this minimum there is always an unstable mode and so the fluid is unstable to infinitesimal disturbances. The value of m corresponding to this minimum, and the corresponding Q and ω are, to 4 significant figures,

$$m = 6.244, \quad Q = 147\,700, \quad \omega = 0.6744. \tag{3.23a–c}$$

We have shown previously that, for marginal stability, ω can never be zero. This is confirmed by these results and we see from figure 1(b) that ω is always positive. The disturbances are not stationary in space but move with a downwards phase velocity, ω/m.

The streamlines and the temperature and salinity perturbations corresponding to marginal stability are shown in figure 2. The streamlines in figure 2(a) show how the

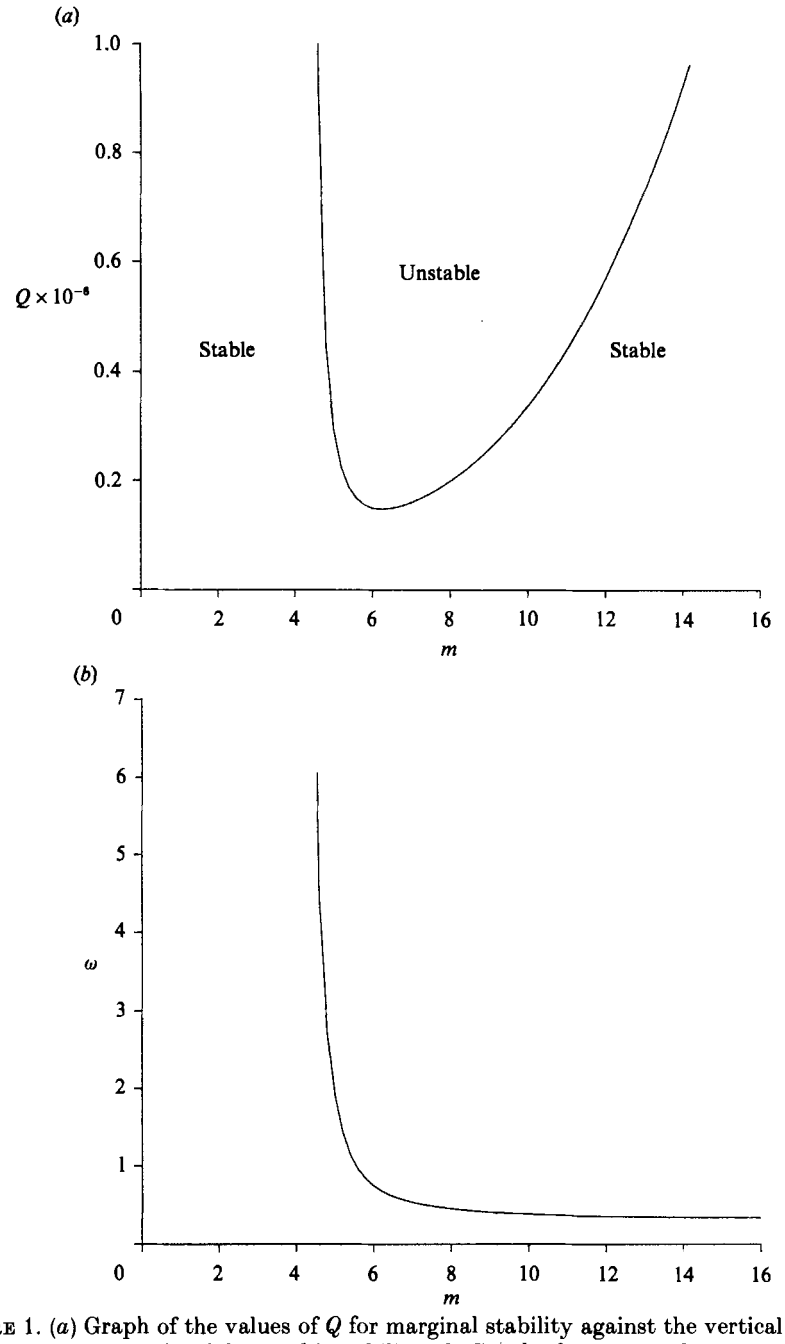

FIGURE 1. (*a*) Graph of the values of Q for marginal stability against the vertical wavenumber m, showing the regions of stability and instability. (*b*) Graph of ω against the vertical wavenumber m for the cases of marginal stability.

linear stability theory predicts a series of counter-rotating convective cells that slope down away from the wall. This slope is due to the fluid moving away from the wall being warmer and saltier than the fluid at an equivalent level further from the wall. As it moves from the wall it moves into cooler fluid and loses its heat faster than it loses its salt. The fluid then becomes heavier than the surrounding fluid and tends to

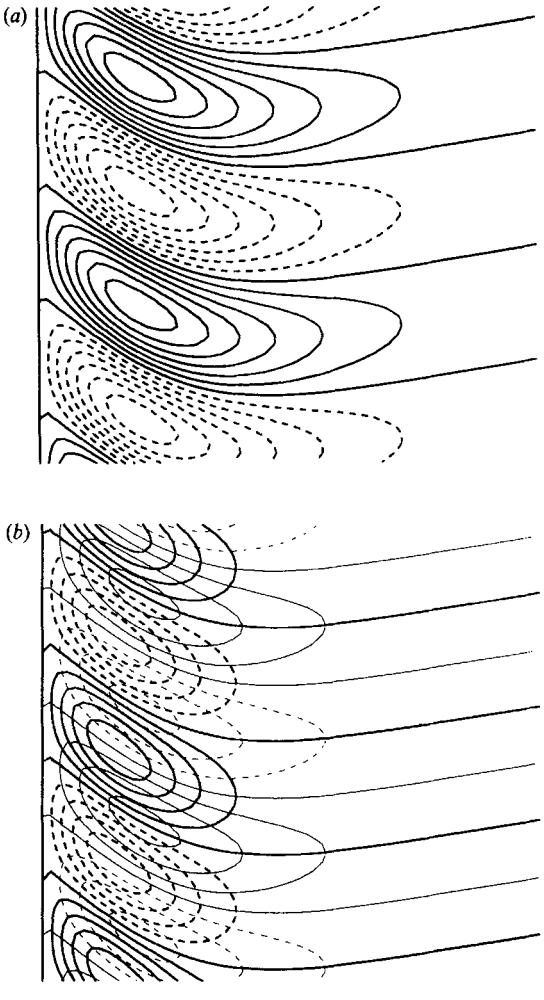

FIGURE 2(a, b). For caption see facing page.

sink. Similarly the incoming fluid tends to rise. Away from the wall the streamlines tend towards parallel lines of constant slope. In this region there is no active convection. The streamlines indicate the presence of internal waves that are being generated by the moving periodic instabilities at the wall. Since the horizontal components of the group and phase velocities of internal waves point in the same direction, the phase velocity of these waves (perpendicular to their streamlines) points downwards and away from the wall. This confirms that the sign of ω is positive for marginal stability. The temperature perturbations, figure 2(*b*), show the fluid moving away from the wall carrying heat into a cooler environment, while the fluid moving towards the wall is cooler. The salinity perturbations, figure 2(*c*), show the horizontal motions cause similar changes to the salinity, but now the presence of a vertical salinity gradient leads to any vertical velocities also causing a change in the local salt concentration. This can be seen clearly near the wall where upward velocities are associated with increases in the salinity. Note that the perturbations in S are much larger than the perturbations in T, this is due to the large difference between their diffusivities.

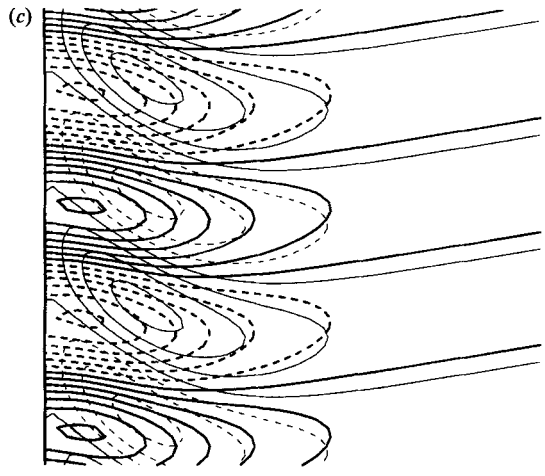

FIGURE 2. (*a*) Plots of the streamlines of the instability at the critical value of Q. Here x is in the range 0 to 6 in the non-dimensional lengthscale, while two complete cycles are plotted in the vertical (roughly a range of 2 in the z-direction). The contours of the stream function are plotted from -0.6 to $+0.6$ in steps of 0.1, the negative contours are dashed. (*b*) Plots of the temperature perturbations, superimposed are the streamlines (the thin lines), for marginal stability. The isotherms are plotted at levels from -0.04 to $+0.04$ in steps of 0.01, the negative isotherms are dashed. (*c*) Plots of the salinity perturbations, superimposed are the streamlines (the thin lines), for marginal stability. The lines of constant salinity perturbation are at levels from -1.2 to $+1.2$ in steps of 0.2, the negative contours are dashed.

We can also look for the growth rate of linear disturbances. If we let λ have a non-zero real part then we gain an extra degree of freedom in the eigenvalue problem. This degree of freedom is taken up by prescribing the value of Q. In the same manner as before we solve the eigenvalue problem to find the real and imaginary parts of λ as functions of Q and m. The results are shown in figure 3. The curves of constant growth rate in figure 3(*a*) have minima that shift to the right as the value of the growth rate increases. Each minimum corresponds to the fastest growing mode for any given value of Q and so this shows that the wavenumber of the fastest growing mode increases as the value of Q increases. Comparing the contours of ω in figure 3(*b*) with figure 3(*a*) we see that as the heating rate Q increases the value of ω corresponding to the fastest growing mode also increases. However, looking at the relative sizes of the growth rate $\mathrm{Re}\{\lambda\}$ and ω in figure 3(*c*) we see that the ratio of $\mathrm{Re}\{\lambda\}$ to ω becomes larger for the fastest growing mode as the value of Q increases.

Up to this point the calculations all use $\sigma = 7$ and $\tau = \frac{1}{80}$, the approximate values for heat and salt in water. For different fluids and solutes the values of σ and τ can vary greatly from these values. By the convention that of the two components that effect the density the one that diffuses faster is called the heat and the slower component the salinity, in all cases $\tau < 1$. With this convention in mind the critical values of Q, and the corresponding values of m and ω, were calculated for values of σ between 0.01 and 100 and for values of τ between 0.001 and 1. The results are shown in figure 4. These plots show a reflective symmetry about the line $\sigma = \tau$. This is due to (3.20) being invariant to interchanges of σ and τ. The inclusion of the $(1-\tau)$ factors in the definition of Q and the vertical lengthscale (and hence in the timescale) has the result that the critical values of all three quantities do not have singularities as τ approaches 1. The plots also show that for $\sigma > 1$, Q only varies by a small amount for large variations in σ and τ, and that as σ gets larger the dependency of

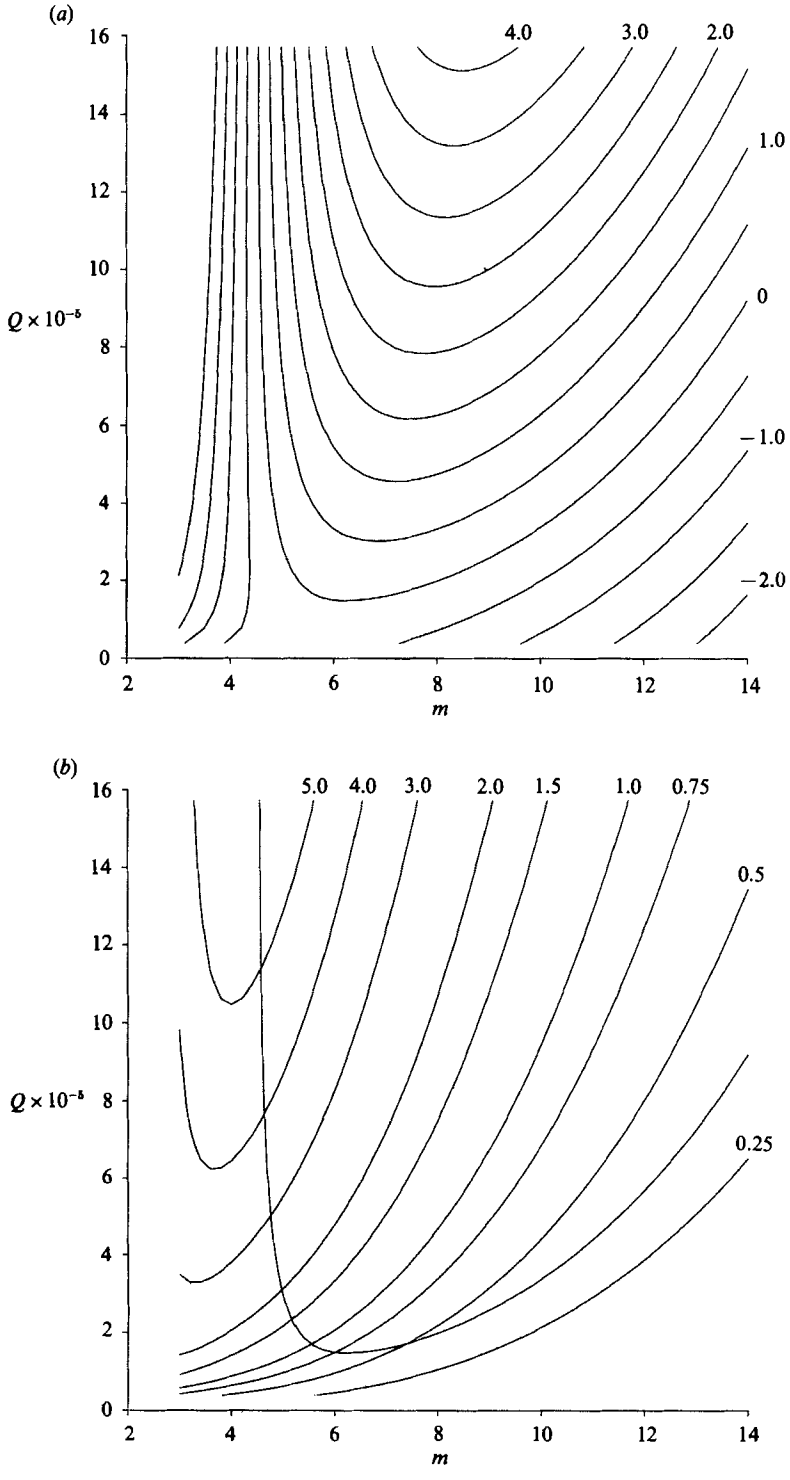

FIGURE 3(a, b). For caption see facing page.

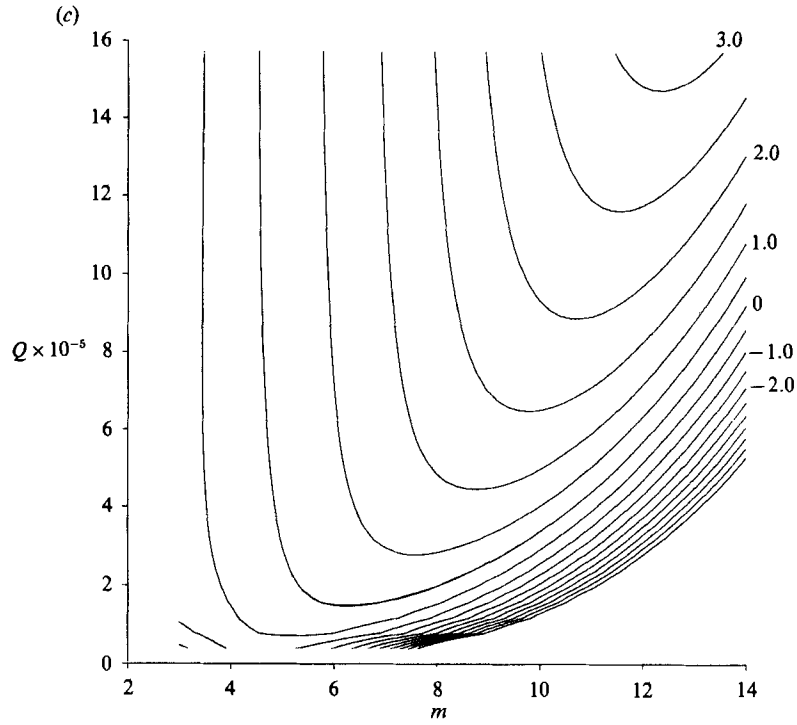

FIGURE 3. Contours of the values of (*a*) $\mathrm{Re}\{\lambda\}$, (*b*) $\omega = \mathrm{Im}(\lambda)$ and (*c*) $\mathrm{Re}\{\lambda\}/\omega$ for values of Q between 0 and 16×10^5 and for m between 3 and 14. The contours are plotted for (*a*) values of $\mathrm{Re}\{\lambda\}$ in the range of -2 to 4 with intervals of 0.5. (*b*) ω taking the values 0.25, 0.5, 0.75, 1.0, 1.5, 2.0, 3.0, 4.0 and 5.0 and (*c*) values of $\mathrm{Re}\{\lambda\}/\omega$ in the range -5 to 3 with intervals of 0.5.

Q on σ becomes weaker. This σ independence is also seen in the results for ω and m in figures 4(*b*) and 4(*c*). For the most unstable modes, as σ becomes very large the convection rolls are still limited in height by the vertical lengthscale, and so m will remain of order 1. Also, we would not expect ω to become much larger as the viscosity increased. Thus we would expect that as σ becomes larger the factor $(\mathrm{i}\omega + \sigma m^2)$ in (3.20) could be approximated by σm^2, and so the Prandtl number will cancel out to leading order leaving the equation for ψ independent of σ. In this limit of large σ the equation for ψ is

$$0 = \psi'' + \frac{\mathrm{i}m^3(\psi f')'}{(\mathrm{i}\omega + m^2)} - \frac{m^4(\mathrm{i}\omega + \tau m^2)}{\tau Q}\psi. \tag{3.24}$$

If we look at the behaviour as $\tau \to 0$ we find that to leading order ω is proportional to τ, and so we define $\hat{\omega}$ by

$$\omega = \tau\hat{\omega}. \tag{3.25}$$

Substituting this into (3.24) we find that, neglecting terms of order τ,

$$0 = \psi'' + \mathrm{i}m(\psi f')' - \frac{m^4(\mathrm{i}\hat{\omega} + m^2)}{Q}\psi. \tag{3.26}$$

This can be solved numerically to find the minimum value of Q, and the corresponding

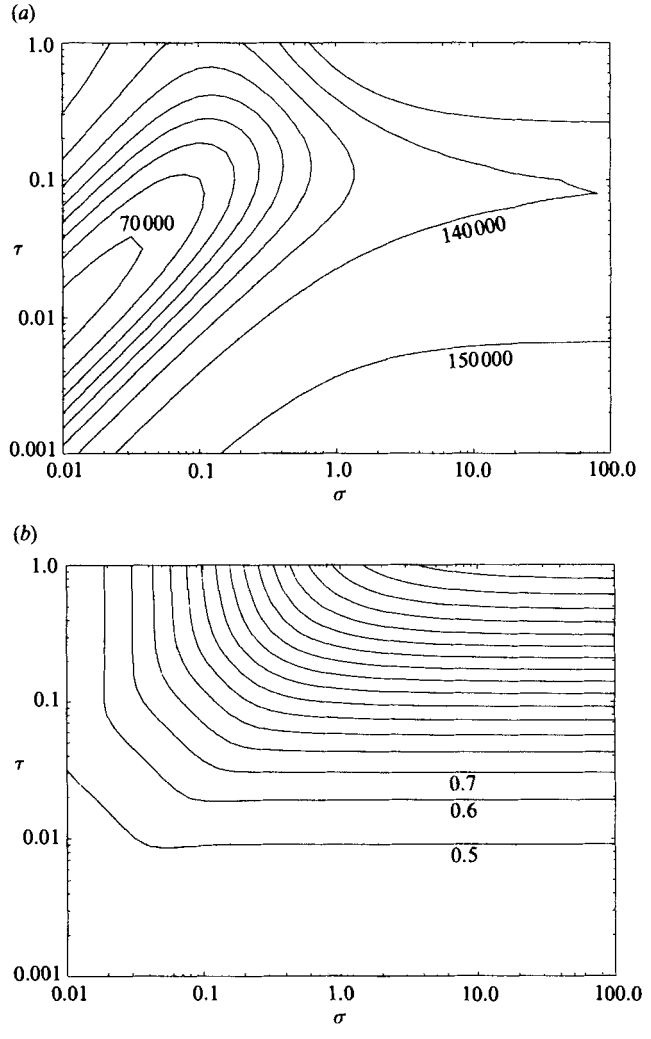

FIGURE 4 (a, b). For caption see facing page.

value of $\hat{\omega}$, as before. From this we obtain the result that for $\sigma \gg 1$ and $\tau \ll 1$ the values of Q, ω and m at the critical point are

$$Q = 152500, \quad \omega = 56.88\tau, \quad m = 6.375. \tag{3.27a–c}$$

In the results shown in figure 4 it can also be seen that in the region where both σ and τ are small the values of Q and m do not change significantly along the line $\sigma = \tau$. In the neighbourhood of this line the contours of Q and m are nearly parallel. However, ω decreases along this line, behaving approximately as $(\sigma\tau)^{\frac{1}{2}}$. In this limit (3.20) becomes, to leading order,

$$0 = \psi'' + \mathrm{i}m(\psi f')' - \frac{m^2(\mathrm{i}\omega + \tau m^2)(\mathrm{i}\omega + \sigma m^2)}{\tau\sigma Q}\psi. \tag{3.28}$$

If we rescale ω by a factor of $(\sigma\tau)^{\frac{1}{2}}$, setting

$$\omega = (\sigma\tau)^{\frac{1}{2}}\omega^*, \tag{3.29}$$

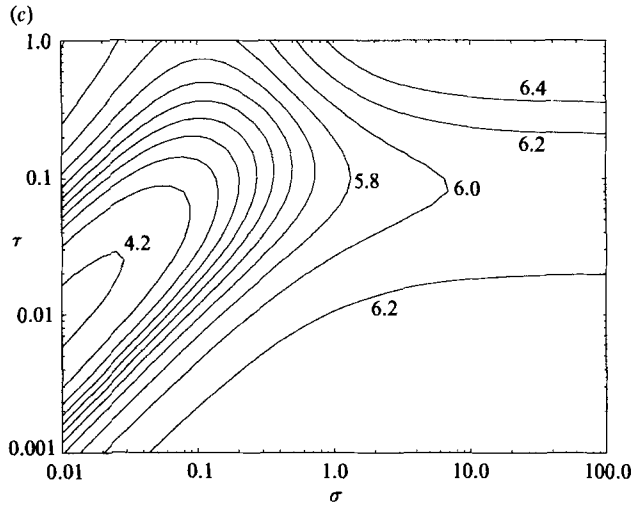

FIGURE 4. (*a*) Contours of the critical values of Q for values of σ between 0.01 and 100, and for values of τ between 1 and 0.001. The contour levels range from 70000 to 150000 in steps of 10000. (*b*) Contours of ω corresponding to the critical values of Q for values of σ between 0.01 and 100, and for values of τ between 1 and 0.001. The contour levels go from 0.5 to 8.5 in steps of 0.5. (*c*) Contours of m corresponding to the critical values of Q for values of σ between 0.01 and 100, and for values of τ between 1 and 0.001. The contour levels go from 4.2 to 6.4 in steps of 0.2.

then (3.28) becomes

$$0 = \psi'' + \mathrm{i}m(\psi f')' - \frac{m^2}{Q}\left(m^4 - \omega^{*2} + \mathrm{i}\omega^*\left(\frac{\sigma^{\frac{1}{2}}}{\tau^{\frac{1}{2}}} + \frac{\tau^{\frac{1}{2}}}{\sigma^{\frac{1}{2}}}\right)\right)\psi. \tag{3.30}$$

In this equation σ and τ only appear in the term $((\sigma^{\frac{1}{2}}/\tau^{\frac{1}{2}}) + (\tau^{\frac{1}{2}}/\sigma^{\frac{1}{2}}))$. This is a function of the ratio of σ and τ. Hence the solutions will only depend on the distance from the line $\sigma = \tau$ on the log–log plots, which is equal to $2^{-\frac{1}{2}}|\log_{10}(\sigma/\tau)|$, resulting in the contours being approximately parallel to the line $\sigma = \tau$.

We can solve (3.30) numerically to find Q, ω^* and m as functions of $|\log_{10}(\sigma/\tau)|$. The results are shown in figure 5. The graph of Q, figure 5(*a*), shows that there is a dip in the critical value of Q when the value of $|\log_{10}(\sigma/\tau)|$ is less than about 2, reaching a low value where $\sigma = \tau$. Outside this region Q rises to a level similar to that found in the large σ case. A similar dip is also found for the critical value of m in figure 5(*c*), although not of the same magnitude. In figure 5(*b*) we see that ω^* has an almost flat region when σ and τ are of similar magnitude, while away from this region the graph drops away. The decay rate in this region is proportional to $(\sigma/\tau)^{\pm\frac{1}{2}}$, the sign being chosen so that this quantity decays as $|\log_{10}(\sigma/\tau)|$ increases. Again this fits in with the large σ region since in this region ω is almost independent of σ and so from the graph we get $\omega(\sigma\tau)^{-\frac{1}{2}}$ behaving like $\tau^{\frac{1}{2}}$. This means that ω will be proportional to τ as $\tau \to 0$.

4. Experimental comparison

In this section we compare the experimental results of Chen *et al.* (1971) and Tsinober & Tanny (1986) relating to the heating of a salinity gradient from a sidewall with the linear theory of the previous section. In the experiments of Chen *et al.* and most of those of Tsinober & Tanny the wall temperature is increased to a

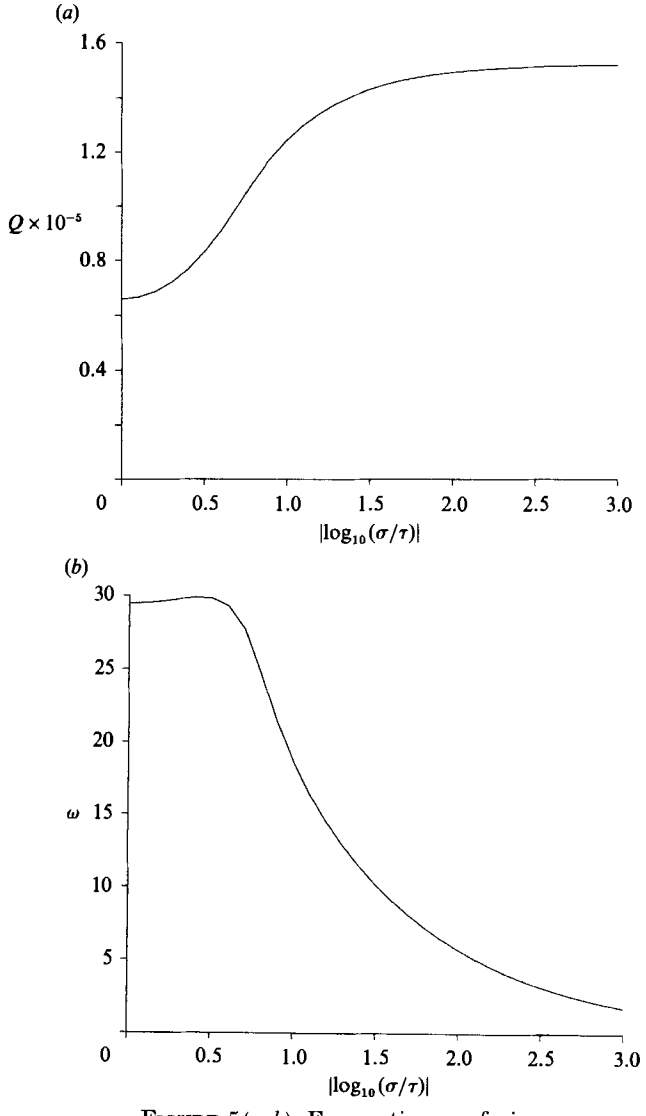

FIGURE 5(a, b). For caption see facing page.

predetermined final level over a timescale of several minutes, with the wall temperature behaving approximately as (2.8). In the experiments of Chen *et al.* s^{-1} was about 3 min, while in those of Tsinober & Tanny they were able to vary its value in the range 75–8000 s. This evolution of the temperature is important since in the linear theory of the previous section we used an error function temperature profile caused by an instantaneous temperature rise of the wall. In this case Q is proportional to $1/t$, where t is the elapsed time since the onset of the wall heating. This results in an initially infinite value of Q which would imply that for sufficiently small time the fluid will always be unstable according to the previous linear theory. However, for small time the value of δ^2 will not be small and so the previous analysis is not valid. The instabilities associated with an instantaneous increase in the wall temperature in a vertical slot was investigated numerically by Chen (1974). If,

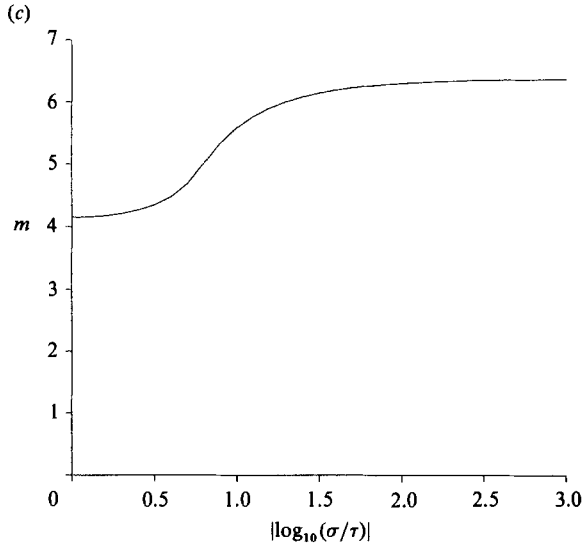

FIGURE 5. (*a*) Graph of the critical value of Q against $|\log_{10}(\sigma/\tau)|$ for the limit of $\sigma \ll 1$ and $\tau \ll 1$. (*b*) Graph of $\omega^* = \omega(\sigma\tau)^{-\frac{1}{4}}$, corresponding to the critical value of Q, against $|\log_{10}(\sigma/\tau)|$ for the limit of $\sigma \ll 1$ and $\tau \ll 1$. (*c*) Graph of m, corresponding to the critical value of Q, against $|\log_{10}(\sigma/\tau)|$ for the limit of $\sigma \ll 1$ and $\tau \ll 1$.

instead, we define Q in terms of the instantaneous wall temperature of the experiments of Chen *et al.* we have

$$Q = \frac{(1-\tau)^6 g(\alpha \Delta T(1-\exp(-st)))^6}{\nu \kappa_S \kappa_T t(-\beta \bar{S}_z)^5}. \tag{4.1}$$

For small time Q is proportional to t^5 and so the fluid starts in a stable regime. As t becomes large Q eventually decays like $1/t$ and so it becomes more stable. From this we see that Q will have a maximum value for some intermediate time. The fluid will not be at its most unstable at this maximum value of Q because the shape of the temperature profile, $f(x)$, also varies with time, giving rise to an increase in the critical value of Q as st increases. Using the temperature profile for this wall temperature, (2.9), we can find the critical values for Q as a function of st, and so find the conditions that ΔT must satisfy for the fluid to be unstable at some time after the initiation of the wall heating. The results are shown in figure 6. This shows how the critical value of Q for each temperature profile that occurs as st increases. The dashed line shows how the time varying Q of (4.1) behaves for the case where it just touches the critical Q curve. The point of contact occurs when

$$st = 2.851. \tag{4.2}$$

At this time the corresponding values of Q and m are

$$Q = 121\,100, \quad m = 6.965. \tag{4.3a–b}$$

Here the vertical distance has been non-dimensionalized with respect to the final wall temperature. From this we can see that the fluid will be unstable at some time if Q exceeds the critical value (4.3*a*) where Q is evaluated when $st = 2.851$.

We can calculate the instantaneous value of Q from the experimental data of Chen *et al.* for each of their experiments for the time when the fluid is most unstable, and

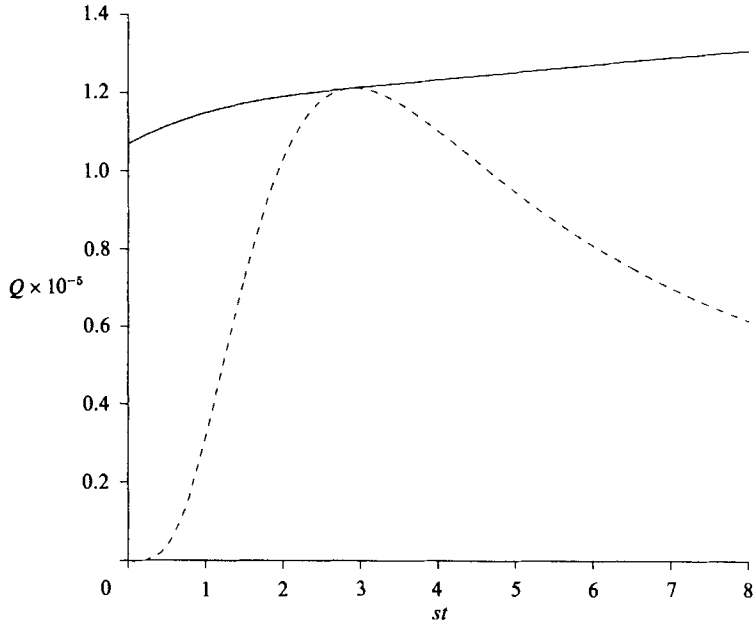

FIGURE 6. Graph of the values of the critical values of Q as the value of st increases (solid line) with the instantaneous values of Q for the wall heating used by Chen *et al.* (1971) (dashed line) for the case where the two curves just touch.

compare the observed stability with the calculated value of the critical Q. The results are shown in table 1. This table gives the calculated value of Q for each experiment. The column marked layer depth gives the average thickness of the observed layers non-dimensionalized with respect to the vertical lengthscale h'. These layer depths are only given for test runs where the instabilities were observed on the whole sidewall. If this did not occur the run was deemed to be subcritical. The last column gives the Rayleigh number,

$$Ra = \frac{g\alpha \Delta T h'^3}{\nu \kappa_T}, \tag{4.4}$$

that they calculated for each test. At first glance these results may not seem too encouraging since some tests were deemed subcritical when the linear theory predicts that they should be supercritical. However, Chen *et al.* observed that some of the tests that were subcritical had instabilities that formed at the top and bottom of the tank first. Further instabilities then appeared near the bottom of the wall, with the region of instability growing upwards. The first of these effects they ascribe to the reduced vertical salinity gradients at the top and bottom boundaries. If instead of applying the stability criterion globally we apply it locally then this would fit in with the predictions of the linear stability analysis since the local salinity gradient was reduced near the top and bottom boundaries in their experiments. The second of these effects they ascribe to an interaction between the lower layers that induces the motion at higher levels. If this was the cause then it would be expected that at marginal stability the group velocity $(-\partial\omega/\partial m)$ of the disturbances would be comparable to the rate of propagation of this front. Examination of figure 3(b) in the neighbourhood of the critical point shows that the group velocity is indeed positive and so the waves would propagate upwards, but the value of the group velocity is not

Test number	Q	Layer depth	Ra
1	3920	Subcritical	800
2	4840	Subcritical	900
3	55800	Subcritical	4500
8	225000	Subcritical	11300
6	315000	0.907	14200
5	348000	Subcritical	15200
9	374000	Subcritical	15700
11	451000	0.756	18100
14	564000	0.837	24400
12	609000	0.847	25500
13	633000	0.835	25400
10	923000	0.689	26800
15	1810000	0.973	53900
7	1920000	0.747	44000
4	2110000	0.674	50500

TABLE 1

very large (about 0.262) and so they would propagate upwards at a similar rate to the rate that heat would diffuse upwards. In the experiments the disturbances are observed to propagate faster than this. When we apply a local stability criterion we are able to take into account the nonlinearity of the equation of state for the fluid, since the linear approximation (2.2) is not a good approximation for the large variations of salinity that occur over the whole tank, although the linear approximation will still be appropriate on the lengthscale associated with the instabilities. Using the nonlinear equation of state from Ruddick & Shirtcliffe (1979) we can calculate how the local value of Q varies with depth in the experiments. Two examples of how Q varies with height are shown in figure 7. The first of these is for test number 3 of Chen *et al.* Even though the local value of Q at the midpoint of the tank is less than half the critical value there is a region near the bottom boundary that is locally unstable. This region occupies about a fifth of the height of the tank. Chen *et al.* show some photographs of this experiment in their figure 6 (these photographs have been published upside down). In the middle of the three photographs, taken after 10 minutes, convection cells are visible in the lower fifth of the tank, just after the linear theory predicts that the water should be at its most unstable. The second example, figure 7(*b*), shows test number 6, the test with the lowest value of Q that was supercritical. Although the value of Q at the midpoint is about two and a half times the critical value, at the top of the tank the water is only just unstable. However there is not perfect agreement with all of the examples, tests 5 and 9 also have supercritical values of Q at all heights, but both were found to be subcritical by Chen *et al.* All the other tests agreed with expectations, tests 1 and 2 were subcritical at all points, test 8 was supercritical for all but a small section near the surface where it was subcritical, and the rest were supercritical at all heights.

One feature that all of the experiments had in common was the large difference in the local values of Q between the surface and the bottom. In most cases the ratio between the top value and the bottom value was about 8. From this we would expect that, even if the convection cells had no interaction, the disturbances would appear at the bottom first, and then start 'propagating' upwards. This can be seen in their figure 8 which shows photographs of tests 9 and 12. This removes the need to consider some form of propagating front to the instabilities as suggested by Thorpe *et al.*

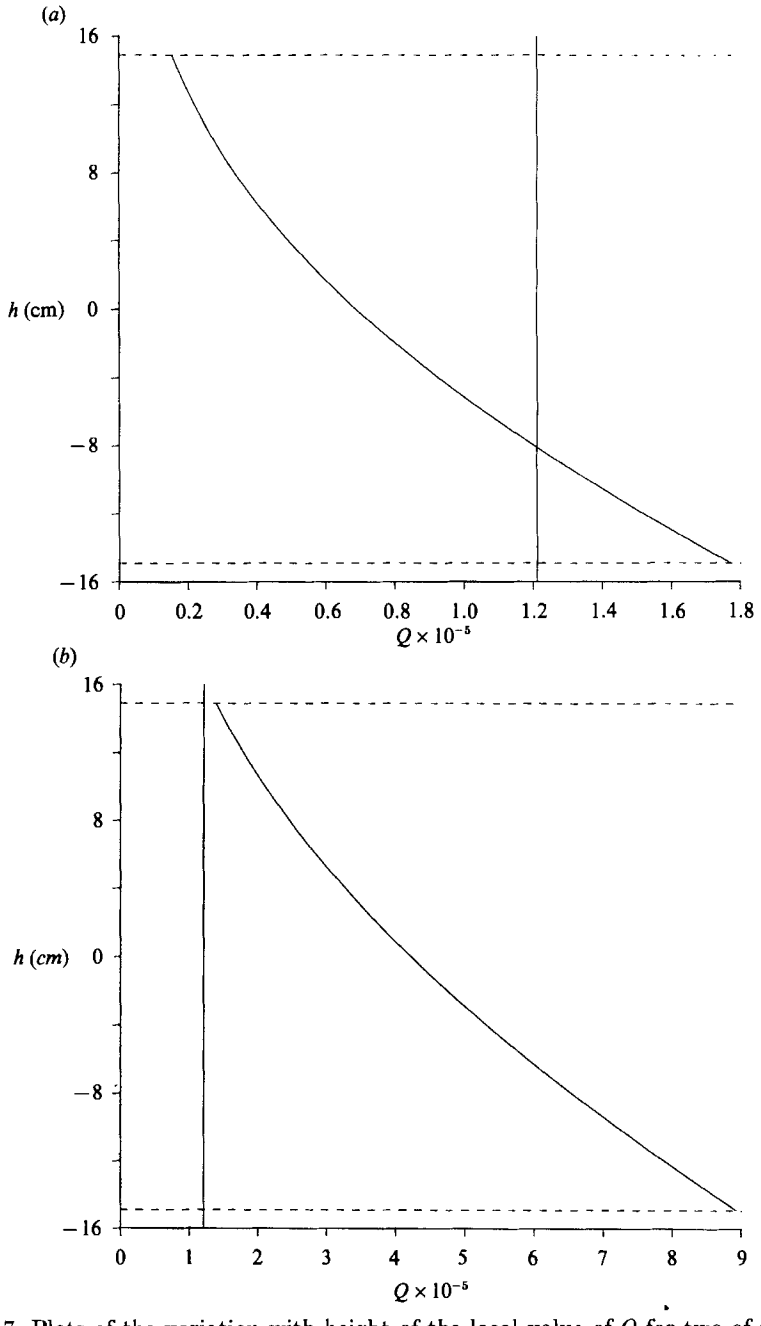

FIGURE 7. Plots of the variation with height of the local value of Q for two of the tests of Chen *et al.* (1971); (*a*) shows test 3 and (*b*) shows test 6. The vertical line is the critical value of Q from the linear theory.

In the experiments of Tsinober & Tanny it was possible to control the time variation of the wall temperature. They used two different time dependencies for the wall temperature. For compatibility with Chen *et al.* they used (2.8) as a condition for the wall temperature for most of their experiments. In addition they also conducted some experiments in which the rise in the wall temperature was

proportional to time. They monitored the wall temperature and recorded its value at the point when the instabilities were first observed at the centre of the heated wall. With this information they were able to make a plot of the points where the experiments went unstable on a Ra_T versus Ra_S graph, where Ra_T and Ra_S are defined by

$$Ra_T = \frac{g\alpha\,\Delta T d^3}{\nu\kappa_T}, \quad Ra_S = \frac{g\beta\bar{S}_z d^4}{\nu\kappa_T}, \tag{4.5}$$

where d is the horizontal lengthscale $(\kappa_T t)^{\frac{1}{2}}$. These non-dimensional numbers were evaluated using the values of the parameters at the centre of the wall. By using a stability criterion based on the centre of the wall they eliminated the problems due to the nonlinearity of the equation of state.

We can use the linear theory to predict a band in the (Ra_T, Ra_S)-plane in which these experiments should become unstable when the salinity gradient is sufficiently strong. The first limit to look at is the case where the wall temperature is proportional to time. For the non-dimensionalization we have taken the reference temperature to be the instantaneous value at the wall. With the corresponding temperature profile, (2.10), we can calculate the critical values of Q, m and ω for this case:

$$Q_1 = 107\,000, \quad m_1 = 7.193, \quad \omega_1 = 0.9225. \tag{4.6a–c}$$

Here we have used the instantaneous vertical lengthscale for the non-dimensionalization of m_1 and ω_1. Since we are using the instantaneous values of the wall temperature we find that for each experiment Q_1 is a function of the elapsed time. As the wall temperature is proportional to t the value of Q for each experiment increases as t^5. From this we can see that eventually Q will reach the critical value in any experiment. This value of Q_1 tells us the time when the instabilities will first appear. We can use the formula for Q_1, Ra_T and Ra_S at this point of instability to give an expression for Ra_T in terms of Ra_S at this critical point:

$$Ra_T = \frac{\tau^{\frac{1}{6}}}{(1-\tau)} Q_1^{\frac{1}{6}} Ra_S^{\frac{5}{6}}. \tag{4.7}$$

Note that this expression is independent of the rate of change of wall temperature.

The second limit that we need to find corresponds to experiments that only just become unstable. If we look at how any experiment progresses on the (Ra_T, Ra_S)-plane we see that for small values of st, Ra_T is proportional to $t^{\frac{5}{2}}$ and Ra_S is proportional to t^2, and so the trajectory of a point corresponding to the current state of the experiment moves upwards with a gradient of 5/4, greater than that of the line of marginal stability. For large values of st we find that the trajectory moves with a gradient of 3/4, less than that of the line of marginal stability. The point on this trajectory that corresponds to marginal stability is the point found previously in the examination of the experiments of Chen *et al.* with Q given by (4.3a), and so we let

$$Q_2 = 121\,100. \tag{4.8}$$

As before, we can find a relationship between Ra_T and Ra_S corresponding to this critical point:

$$Ra_T = \frac{\tau^{\frac{1}{6}}}{(1-\tau)} Q_2^{\frac{1}{6}} Ra_S^{\frac{5}{6}}. \tag{4.9}$$

Again, this is independent of the rate of wall heating.

When the fluid is heated with a Chen *et al.* type wall temperature it can become unstable for any value of st up to 2.851. The critical values of Q for values of st up

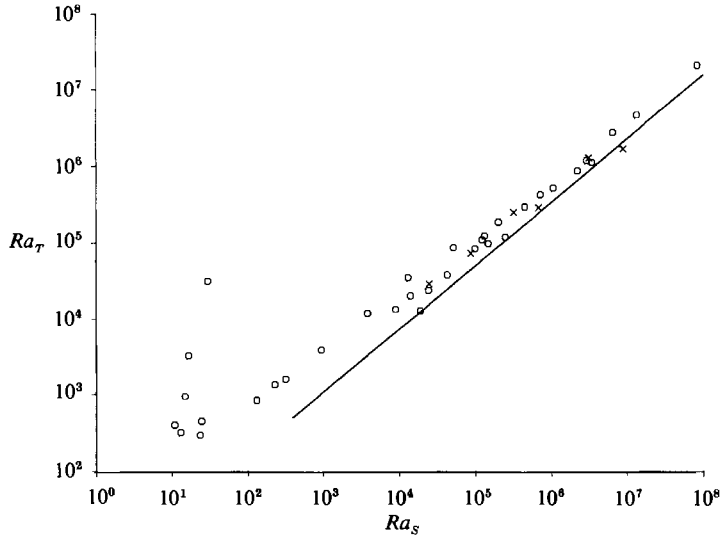

FIGURE 8. Comparison of the linear theory to the experimental results of Tsinober & Tanny (1986) for the heating of a salinity gradient from a single sidewall. The points at which the experiments became unstable, ○, for wall-temperature evolution of the form $T_{\text{wall}} = \Delta T(1-\exp(-st))$; ×, for wall temperature proportional to the elapsed time. The line indicates the position of the band (4.10) above which linear theory predicts that the fluid is unstable. The linear theory is only valid for the larger values of Ra_S.

to this value have already been found. In the limit $st \to 0$ the temperature profile is the same as that due to the wall temperature being proportional to time, (2.10). If the experiment becomes marginally unstable then the value Q at this point will lie between Q_1 and Q_2 and the corresponding Ra_T will lie between the two respective extremes given above. Hence, at the point of instability,

$$\frac{\tau^{\frac{1}{6}}}{(1-\tau)} Q_1^{\frac{1}{6}} Ra_S^{\frac{5}{6}} < Ra_T < \frac{\tau^{\frac{1}{6}}}{(1-\tau)} Q_2^{\frac{1}{6}} Ra_S^{\frac{5}{6}}. \tag{4.10}$$

If this narrow band at which the fluid would be expected to go unstable is superimposed on the Ra_S–Ra_T plot of the experimental results of Tsinober & Tanny for the heating of a salinity gradient, figure 8, we find that all bar one of the data points lie above this band. The instabilities can only be observed when the fluid has moved a finite distance, hence there will be a delay between the onset of instability and the observation and registration of the data points. For this reason the band should give a lower bound for the data points and not a line through their middle. This band does indeed give a good lower bound for the data points. For data points below a value of Ra_S of about 10000 the agreement is less good. The lower the values of Ra_S correspond to larger values of δ, and so the linear model with its quasi-static assumption breaks down. Tsinober & Tanny also reported that it was harder to judge the exact point of instability for these lower values of Ra_S, giving an error estimate of up to 30% for the values of Ra_T in this region.

When the theory was applied to the experiments of Chen *et al.* and Tsinober & Tanny it predicted the onset of instabilities well. The major discrepancy between the linear theory and the observations was the form of the convection cells. The linear theory, by its nature, predicts counter-rotating convection cells. In all the experiments the observed cells all rotated in the same sense. For convection cells to

be observed they must be of finite amplitude, and so nonlinear effects will be important once they have developed. These nonlinear effects are beyond the scope of this linear theory, and some of their aspects are examined in Kerr (1989).

5. Boundary-layer calculations

In §3 we derived the equations of motion for the instabilities caused by the heating of a salinity gradient from a sidewall, and looked at the limit where the horizontal diffusion is neglected. This limit corresponds to taking $\delta = 0$ in (3.6). However, in this limit it is not possible to satisfy all the boundary conditions, in particular we have to drop the no-slip condition and the salt boundary condition at the wall. In reality δ is never zero and in this section we investigate the effect on marginal stability of the flow of retaining a small, but non-zero, δ. In this case the horizontal diffusion has very little effect, except in a boundary layer near the wall where it will be significant. This is equivalent to the extension of the original stability analysis of Thorpe *et al.* (1969) by Hart (1971) for the case of a vertical slot.

We are concerned with solutions that are periodic with respect to both z and t as before, with vertical wavenumber m and frequency ω. To find the horizontal lengthscales that correspond to the boundary layers we rescale the horizontal coordinate in the complete linear non-dimensional equations of motion, (3.6), setting $x = \delta^{\alpha} x'$. There are three values of α which give different non-trivial balances between the leading-order terms in the equations, with $\alpha = 0$, $\alpha = 1$ and $\alpha = \frac{3}{2}$. We will refer to the three regions that correspond to these scalings as the outer, middle and inner layers respectively. In each of these separate regions we find the asymptotic behaviour of ψ, T and S in the limit of small δ and then join the solutions together using the method of matched asymptotic expansions. The wall boundary conditions that are applied in the inner layer are

$$\psi(0) = \frac{\partial \psi(0)}{\partial x} = T(0) = \frac{\partial S(0)}{\partial x} = 0. \tag{5.1}$$

The boundary conditions imposed far from the wall are that all the perturbations decay as $x \to \infty$.

The leading-order solutions in the inner and middle regions are

Inner layer ($x = \delta^{\frac{3}{2}} x''$):

$$\psi = \delta^{1\frac{1}{2}} \frac{(\mathrm{i}\omega + \tau m^2)}{(1-\tau)} A_{\mathrm{i}} \left(x'' - \frac{\sin(Mx'')}{M} \mathrm{e}^{-Mx''} \right) + \frac{\tau \delta^{\frac{1}{2}}}{(1-\tau)} B_{\mathrm{i}} (1 - \cos(Mx'') \mathrm{e}^{-Mx''} - \sin(Mx'') \mathrm{e}^{-Mx''}) \tag{5.2a}$$

$$T = B_{\mathrm{i}} x'', \tag{5.2b}$$

$$S = A_{\mathrm{i}} + \delta \frac{(\mathrm{i}\omega + \tau m^2)}{2\tau M^2} A_{\mathrm{i}} (1 - \cos(Mx'') \mathrm{e}^{-Mx''} - \sin(Mx'') \mathrm{e}^{-Mx''}) + B_{\mathrm{i}} \left(x'' + \frac{\cos(Mx'')}{M} \mathrm{e}^{-Mx''} \right), \tag{5.2c}$$

where

$$M^4 = \tfrac{1}{4} Q. \tag{5.3}$$

Middle layer ($x = \delta x'$):

$$\psi = A_{\mathrm{m}} + \delta \frac{(\mathrm{i}\omega + \tau m^2)}{(1-\tau)} C_{\mathrm{m}} x', \tag{5.4a}$$

$$T = B_{\mathrm{m}} \exp\left(-(\mathrm{i}\omega + m^2)^{\frac{1}{2}} x'\right) + \frac{\mathrm{i}mf'(0)}{(\mathrm{i}\omega + m^2)} A_{\mathrm{m}} + \frac{\mathrm{i}m\delta(\mathrm{i}\omega + \tau m^2)}{(1-\tau)(\mathrm{i}\omega + m^2)} C_{\mathrm{m}} f'(0)\, x', \tag{5.4b}$$

$$S = B_{\mathrm{m}} \exp\left(-(\mathrm{i}\omega + m^2)^{\frac{1}{2}} x'\right) + \frac{\mathrm{i}mf'(0)}{(\mathrm{i}\omega + m^2)} A_{\mathrm{m}} + C_{\mathrm{m}} + \frac{\mathrm{i}m\delta(\mathrm{i}\omega + \tau m^2)}{(1-\tau)(\mathrm{i}\omega + m^2)} C_{\mathrm{m}} f'(0)\, x'. \tag{5.4c}$$

Matching the inner and middle regions to the outer region, with the extra condition imposed in §3 that in the outer layer the x-derivative of ψ tends to 1 as $x \to 0$, gives the values of the undetermined constants to be

$$A_{\mathrm{i}} = C_{\mathrm{m}} = \frac{(1-\tau)}{(\mathrm{i}\omega + \tau m^2)}, \quad B_{\mathrm{i}} = \delta^{1\frac{1}{2}} \frac{\mathrm{i}mf'(0)}{(\mathrm{i}\omega + m^2)},$$

$$A_{\mathrm{m}} = \sigma^2 \frac{\mathrm{i}mM\tau f'(0)}{(1-\tau)(\mathrm{i}\omega + m^2)}, \quad B_{\mathrm{m}} = \delta^2 \frac{\mathrm{i}m^2 M\tau f'(0)}{(1-\tau)(\mathrm{i}\omega + m^2)^2}. \tag{5.5}$$

The outer layer involves no rescaling and represents the bulk of the fluid. For this layer the governing equations are (3.6). Since the only powers of δ that appear in these equations and the boundary conditions found by matching with the middle layer are multiples of two we can expand ψ, T, S, Q and ω as asymptotic power series in δ^2:

$$\{\psi(x), T(x), S(x)\} = \{\psi_0(x), T_0(x), S_0(x)\} + \delta^2\{\psi_2(x), T_2(x), S_2(x)\} + \ldots,$$

$$\{Q, \omega\} = \{Q_0, \omega_0\} + \delta^2\{Q_2, \omega_2\} + \ldots. \tag{5.6}$$

Substituting these expansions into (3.6) we recover at leading order the equation (3.18) with the boundary conditions that $\psi(0) \to 0$ and $\psi'(0) \to 1$ as $x \to 0$, and that $\psi(x) \to 0$ as $x \to \infty$. The leading-order outer solution is just the solution found previously.

We can extend this analysis in the outer region to calculate the order δ^2 perturbations. The equations for ψ_2, T_2 and S_2 are

$$(\mathrm{i}\omega_0 + \sigma m^2) m^2 \psi_2 + \frac{\tau\sigma Q_0}{(1-\tau)}\left(\frac{\partial T_2}{\partial x} - \frac{\partial S_2}{\partial x}\right) = -\mathrm{i}\omega_2 m^2 \psi_0 - \frac{\tau\sigma Q_2}{(1-\tau)}\left(\frac{\partial T_0}{\partial x} - \frac{\partial S_0}{\partial x}\right)$$
$$+ (\mathrm{i}\omega_0 + 2\sigma m^2)\frac{\partial^2 \psi_0}{\partial x^2} - \tfrac{1}{2}m^2\left(1 - x\frac{\partial}{\partial x}\right)\psi_0 - \mathrm{i}m^3 \bar{w}(x)\,\psi_0, \tag{5.7a}$$

$$(\mathrm{i}\omega_0 + m^2) T_2 - \mathrm{i}mf'(x)\,\psi_2 = -\mathrm{i}\omega_2 T_0 - \mathrm{i}m\bar{w}(x)\,T_0 + \left(\tfrac{1}{2}x\frac{\partial}{\partial x} + \frac{\partial^2}{\partial x^2}\right)T_0, \tag{5.7b}$$

$$(\mathrm{i}\omega_0 + \tau m^2) S_2 - \mathrm{i}mf'(x)\,\psi_2 - (1-\tau)\frac{\partial \psi_2}{\partial x} = -\mathrm{i}\omega_2 S_0 - \mathrm{i}m\bar{w}(x)\,S_0 + \left(\tfrac{1}{2}x\frac{\partial}{\partial x} + \tau\frac{\partial^2}{\partial x^2}\right)S_0. \tag{5.7c}$$

The boundary conditions for ψ_2 and T_2 as $x \to 0$ are

$$\psi_2(0) = \frac{\mathrm{i}m\tau Mf'(0)}{(1-\tau)(\mathrm{i}\omega_0 + m^2)}, \quad T_2(0) = -\frac{m^2\tau Mf'(0)^2}{(1-\tau)(\mathrm{i}\omega_0 + m^2)^2}. \tag{5.8a, b}$$

These two boundary conditions are equivalent. As before we require that the solution decays as $x \to \infty$.

Equations (5.7) do not, in general, have a solution. To find out when a solution does exist we apply a solvability condition. This condition is obtained by finding the adjoints $\hat{\psi}$, $\hat{T}$ and $\hat{S}$ to ψ_0, T_0 and S_0. These satisfy the equations

$$(-\mathrm{i}\omega_0+\sigma m^2)\,m^2\hat{\psi}+(1-\tau)\frac{\partial\hat{S}}{\partial x}+\mathrm{i}mf'(x)\,\hat{T}+\mathrm{i}mf'(x)\,\hat{S}=0, \tag{5.9a}$$

$$-\frac{\tau\sigma Q_0}{(1-\tau)}\frac{\partial\hat{\psi}}{\partial x}+(-\mathrm{i}\omega_0+m^2)\,\hat{T}=0, \tag{5.9b}$$

$$\frac{\tau\sigma Q_0}{(1-\tau)}\frac{\partial\hat{\psi}}{\partial x}+(-\mathrm{i}\omega_0+\tau m^2)\,\hat{S}=0. \tag{5.9c}$$

These can be rearranged to give a single equation for $\hat{\psi}$ which is the adjoint of (3.20), and can be solved in a similar fashion. If each of the (5.7) is multiplied by the corresponding complex conjugate of the adjoints $\hat{\psi}$, $\hat{T}$ and $\hat{S}$, and the sum of the three resultant expressions is then integrated from 0 to ∞, the solvability condition is obtained:

$$\begin{aligned}(1-\tau)\,\bar{\hat{S}}(0)\,\psi_2(0) = &-\frac{\tau\sigma Q_2}{(1-\tau)}\int_0^\infty \bar{\hat{\psi}}\left(\frac{\partial T_0}{\partial x}-\frac{\partial S_0}{\partial x}\right)\mathrm{d}x-\mathrm{i}\omega_2\int_0^\infty m^2\bar{\hat{\psi}}\psi_0+\bar{\hat{T}}T_0+\bar{\hat{S}}S_0\,\mathrm{d}x\\
&+\int_0^\infty \bar{\hat{\psi}}\left(-\tfrac{1}{2}m^2\left(1-x\frac{\partial}{\partial x}\right)\psi_0-\mathrm{i}m^3\bar{w}(x)\,\psi_0+(\mathrm{i}\omega_0+2\sigma m^2)\frac{\partial^2\psi_0}{\partial x^2}\right)\mathrm{d}x\\
&+\int_0^\infty \bar{\hat{T}}\left(-\mathrm{i}m\bar{w}(x)\,T_0+\tfrac{1}{2}x\frac{\partial T_0}{\partial x}+\frac{\partial^2 T_0}{\partial x^2}\right)\mathrm{d}x\\
&+\int_0^\infty \bar{\hat{S}}\left(-\mathrm{i}m\bar{w}(x)\,S_0+\tfrac{1}{2}x\frac{\partial S_0}{\partial x}+\tau\frac{\partial^2 S_0}{\partial x^2}\right)\mathrm{d}x.\end{aligned} \tag{5.10}$$

Since Q_2 and ω_2 are both real, taking real and imaginary parts of this equation gives two simultaneous equations for Q_2 and ω_2. From these the values of Q_2 and ω_2 are evaluated at the marginally stable state found previously to give, for the case of $\sigma=7$ and $\tau=\frac{1}{80}$,

$$Q_2=240\,800,\quad \omega_2=0.3262. \tag{5.11a–b}$$

The value of m that corresponds to marginal stability will also be a function of δ^2. This dependency can be found by expanding $\partial Q/\partial m$ as a double power series in δ^2 and the perturbations of m from the critical value found for $\delta=0$. The values of the relevant terms in the expansion can be found to give the value of m for marginal stability to be

$$m=6.244+0.897\delta^2+O(\delta^4). \tag{5.12}$$

The order δ^2 change to the critical value of m only affects the corresponding value of Q to order δ^4 and so the order δ^2 perturbation to Q given in (5.11a) is the leading-order change. This is not the case for the variation of ω. Since $\partial\omega/\partial m\neq 0$ at the critical point, an order δ^2 change in m will cause an order δ^2 change in ω. The value of ω for marginal stability to order δ^2 is found to be

$$\omega=0.6744+0.0911\delta^2+O(\delta^4). \tag{5.13}$$

At this point we must look at these results in the light of the quasi-static assumption made in §3. The justification for that assumption is that the growth rates of the instabilities are much greater than the growth rate of the thermal layer at the

wall. The growth rate of this thermal layer is of order δ^2, while near the critical point the growth rate λ of the instabilities has the relationship

$$\mathrm{Re}\{\lambda\} = O(Q - Q_{\mathrm{crit}}). \tag{5.14}$$

Hence the quasi-static assumption as stated in §3 breaks down when

$$Q - Q_{\mathrm{crit}} = O(\delta^2). \tag{5.15}$$

Although the analysis if strictly speaking invalid for marginal stability, the location of the boundary between stability and instability is found with an error of order δ^2. We find from the boundary-layer calculations that the first influence of horizontal diffusion and the boundary layer has an effect on the critical value of Q of order δ^2, and so these estimates for the variations in the parameters for the critical point for small δ lie within the error limits inherent in the quasi-static assumption. However, they may give an indication as to the possible effects of non-zero δ on the onset of instabilities. The positive value of Q_2 could be interpreted as indicating that the probable effect of the extra horizontal diffusion is to stabilize the fluid, while the positive coefficient of δ^2 in (5.13) would indicate that the frequency of the critical disturbance would increase. However the vertical phase velocity of the disturbances, $-\omega/m$, is only weakly affected by the non-zero δ, being given by

$$-\omega/m = -0.1080 + 0.000\,92\delta^2 + O(\delta^4). \tag{5.16}$$

Thus we may deduce that any effect of a non-zero δ would have little effect on the phase velocity.

It must be emphasized that the results in this section that relate to the effect of a non-zero δ on the parameters Q, m and ω for the critical instabilities do violate the quasi-static assumption, and hence should only be taken as an indication of what the real effects may be. It is beyond the scope of this analysis to take into account properly the effect of the time-dependency of the thermal layer. However, the form of the solutions calculated for the boundary layers of thickness $\delta^{\frac{3}{2}}$ and δ do not require the breaking of the quasi-static assumption and will give the leading-order form of the perturbations in these regions when the conditions for the linear analysis are satisfied.

6. Conclusion

In this paper we have looked at the effect of heating a body of fluid with a vertical salinity gradient from a vertical sidewall. We investigated the linear stability of the resultant temperature and salinity distributions. We found that the relevant non-dimensional number for this configuration is

$$Q = \frac{(1-\tau)^6 g(\alpha \Delta T)^6}{\nu \kappa_S l^2 (-\beta \bar{S}_z)^5}, \tag{6.1}$$

in the case where the ratio between the horizontal lengthscale and the vertical lengthscale is small. It was found that for the case of water the onset of instability occurred when this number was about 148000 for the error-function temperature profile. For all possible values of the diffusivities of heat and salt and values of the viscosity, this parameter varies between about 70000 and 170000 for the onset of instability. This linear theory requires a quasi-static assumption which is equivalent to assuming the vertical lengthscale is much smaller than the horizontal lengthscale. This condition will be satisfied when either the salinity gradient is strong or the

heating rate is slow. This theory predicts the onset of instability in experiments that satisfy these conditions well, and also explains the apparent propagation of instabilities along the heated wall observed by Chen *et al.* (1971). However it does not predict the observed form of the instabilities, which in experiments consist of a series of cells that all rotate in the same direction. The linear theory, by its nature, predicts a series of counter-rotating cells and so a nonlinear treatment of the subject is required to address this phenomenon. Some of the nonlinear aspects of the sidewall heating of a salinity gradient are dealt with in Kerr (1989).

I would like to thank Dr H. E. Huppert for suggesting this subject, and to thank all the other participants of the 1984 Geophysical Fluid Dynamics Summer Program at the Woods Hole Oceanographic Institution for providing me with such an enjoyable and rewarding summer. I would also like to thank Professor A. Tsinober and Dr J. Tanny for the use of their experimental data. Lastly I would also like to thank Dr J. Y. Holyer for many helpful discussions.

Appendix

In the case of an infinite vertical slot with a vertical salt gradient and a linear lateral temperature gradient, as looked at by Thorpe *et al.* (1969) and Hart (1971), the analogous condition to (3.22) is satisfied trivially since $f''(x) = 0$. Since this problem is in a finite slot of non-dimensional width 1 we can replace the boundary condition at infinity with the condition that ψ vanishes at $x = 1$. The equation to solve for this problem would then be

$$0 = \psi'' - \mathrm{i}m\psi' - \frac{m^6}{Q}\psi, \tag{A 1a}$$

with

$$\psi(0) = \psi(1) = 0. \tag{A 1b}$$

This has a solution

$$\psi = A\,\mathrm{e}^{\mathrm{i}ax} + B\,\mathrm{e}^{\mathrm{i}bx}, \tag{A 2}$$

where

$$a = \frac{1}{2}\left(m + \left(m^2 - \frac{4m^6}{Q}\right)^{\frac{1}{2}}\right), \tag{A 3a}$$

and

$$b = \frac{1}{2}\left(m - \left(m^2 - \frac{4m^6}{Q}\right)^{\frac{1}{2}}\right). \tag{A 3b}$$

The boundary condition at $x = 0$ gives $A = -B$, while that at $x = 1$ gives

$$a = b + 2n\pi, \tag{A 4}$$

and so

$$Q = \frac{4m^6}{m^2 - 4n^2\pi^2}. \tag{A 5}$$

This has a minimum when $n = 1$ and so the point of marginal stability is given by

$$m = \sqrt{6}\,\pi, \quad Q = 432\,\pi^4. \tag{A 6}$$

When these results are expressed in terms of parameters used by Thorpe *et al.* (1969), and by Hart (1971) we retrieve the results given for a strong salinity stratification.

REFERENCES

CHEN, C. F. 1974 Onset of cellular convection in a salinity gradient due to a lateral temperature gradient. *J. Fluid Mech.* **63**, 563–576.

CHEN, C. F. 1975 Double-diffusive convection in an inclined slot. *J. Fluid Mech.* **72**, 721–729.

CHEN, C. F., BRIGGS, D. G. & WIRTZ, R. A. 1971 Stability of thermal convection in a salinity gradient due to lateral heating. *Intl J. Heat Mass Transfer* **14**, 57–65.

CHEN, C. F. & SANDFORD, R. D. 1977 Stability of time-dependent double-diffusive convection in an inclined slot. *J. Fluid Mech.* **83**, 83–95.

GILL, A. E. 1966 The boundary-layer regime for convection in a rectangular cavity. *J. Fluid Mech.* **26**, 515–536.

HART, J. E. 1971 On sideways diffusive instability. *J. Fluid Mech.* **49**, 279–288.

HUPPERT, H. E. & JOSBERGER, E. G. 1980 The melting of ice in cold stratified water. *J. Phys. Oceanogr.* **10**, 953–960.

HUPPERT, H. E., KERR, R. C. & HALLWORTH, M. A. 1984 Heating or cooling a stable compositional gradient from the side. *Intl J. Heat Mass Transfer* **27**, 1395–1401.

HUPPERT, H. E. & TURNER, J. S. 1980 Ice blocks melting into a salinity gradient. *J. Fluid Mech.* **100**, 367–384.

KERR, O. S. 1989 Heating a salinity gradient from a vertical sidewall: nonlinear theory. Submitted.

KERR, O. S. & HOLYER, J. Y. 1986 The effect of rotation on double-diffusive interleaving. *J. Fluid Mech.* **162**, 23–33.

LINDEN, P. F. & WEBER, J. E. 1977 The formation of layers in a double-diffusive system with a sloping boundary. *J. Fluid Mech.* **81**, 757–773.

MCDOUGALL, T. J. 1985 Double-diffusive interleaving. Part I: Linear stability analysis. *J. Phys. Oceanogr.* **15**, 1532–1541.

NIINO, H. 1986 A linear theory of double-diffusive horizontal intrusions in a temperature-salinity front. *J. Fluid Mech.* **171**, 71–100.

PALIWAL, R. C. & CHEN, C. F. 1980*a* Double-diffusive instability in an inclined fluid layer. Part 1. Experimental investigation. *J. Fluid Mech.* **98**, 755–768.

PALIWAL, R. C. & CHEN, C. F. 1980*b* Double-diffusive instability in an inclined fluid layer. Part 2. Stability analysis. *J. Fluid Mech.* **98**, 769–785.

RUDDICK, B. R. & SHIRTCLIFFE, T. G. L. 1979 Data for double diffusers: Physical properties of aqueous salt-sugar solutions. *Deep-Sea Res.* **26**, 775–787.

STERN, M. E. 1967 Lateral mixing of water masses. *Deep-Sea Res.* **14**, 747–753.

THANGAM, S., ZEBIB, A. & CHEN, C. F. 1981 Transition from shear to sideways diffusive instability in a vertical slot. *J. Fluid Mech.* **112**, 151–160.

THORPE, S. A., HUTT, P. K. & SOULSBY, R. 1969 The effects of horizontal gradients on thermohaline convection. *J. Fluid Mech.* **38**, 375–400.

TOOLE, J. M. & GEORGI, D. T. 1981 On the dynamics and effects of double-diffusively driven intrusions. *Prog. Oceanogr.* **10**, 123–145.

TSINOBER, A. & TANNY, J. 1986 Visualization of double-diffusive layers. In *Flow Visualization IV* (ed. Claude Venet), pp. 345–351. Hemisphere.

TANNY, J. & TSINOBER, A. B. 1988 The dynamics and structure of double-diffusive layers in sidewall-heating experiments. *J. Fluid Mech.* **196**, 135–156.

TURNER, J. S. 1973 *Buoyancy Effects in Fluids.* Cambridge University Press.